Studies of Geomechanical Properties Using Subsurface Borehole Logging

By

Ramone Mikgail Kok
15113

Dissertation submitted in partial fulfilment of
The requirements for the
Bachelor of Tech (Hons)
(Petroleum Geosciences)
FYP II
May 2014

Universiti Teknologi PETRONAS
Bandar Seri Iskandar
31750 Tronoh
Perak Darul Ridzuan

TABLE OF CONTENTS

CERTIFICATION i

ABSTRACT ii

ACKNOWLEDGEMENT iii

CHAPTER 1: INTRODUCTION 1

1.1. Background of Study 1
1.2. Problem Statement 4
1.3. Objective and Scope of Study 5

CHAPTER 2: LITERATURE REVIEW 6

CHAPTER 3: METHODOLOGY 15

CHAPTER 4: RESULTS AND DISCUSSION 24

CHAPTER 5: CONCLUSION 43

REFERENCES 44

CERTIFICATION OF APPROVAL

Studies of Geomechanical Properties Using Subsurface Borehole Logging

By

Ramone Mikgail Kok
15113

A project dissertation submitted to the
Petroleum Geoscience Programme
Universiti Teknologi PETRONAS
in partial fulfilment of the requirements for the
Bachelor of Technology (Hons)
(Petroleum Geosciences)

Approved by,

_____

Mr. Abdull Halim Abdul

UNIVERSITI TEKNOLOGI PETRONAS

TRONOH, PERAK

MAY 2014

CERTIFICATION OF ORIGINALITY

This is to certify that I am responsible for the work submitted in this project, that the original work is my own except specified in the references and acknowledgements, and the original work contained herein has not been undertaken or done by unspecified sources or persons.

_____

RAMONE MIKGAIL KOK

ABSTRACT

This dissertation aims to address the importance of geomechanical studies not just in the oil and gas industry but also in construction engineering, mining and hydrological industry. There are numerous methods to conduct this study but this project places emphasis on utilizing subsurface borehole data with laboratory data to further validate the findings. Universiti Teknologi PETRONAS is a vast area with impressive state of the art architecture, hence proper geomechanical study of the area is vital since there have never been a study like this conducted before. Two cross sections and a land survey map are constructed to study the local geology of the area. Triaxial compression test, compaction / CBR test and particle size distribution are among the tests conducted to study the compressive strength, elastic constants, stress parameters, grain size and sorting and load bearing capacity of the collected samples. There is an abundance of clay and silt up to 13 meters below ground level and limestone from about 15 meters onwards which is believed to be of Kinta origin. The soil disturbance is caused by mining activities in the past. The soil samples obtained is comprised of mainly poorly sorted gravel on the shallower depth and moderately sorted clay and silt in a slightly deeper depth. The sandy silt sample (CBR value from 10 - 20) located south- east to the Chancellor Hall has a maximum dry density of 1.733 mg/m^3 with optimum moisture content of 18% where its strength is at its highest. The Mohr circle plotted shows that the soil has a cohesion value of $2kN/m^2$, angle of internal friction 26.1º where the maximum shear stress that it can handle is $45kN/m^2$ and maximum normal stress is $87kN/m^2$ before failure.

ACKNOWLEDGEMENT

I would like to express my heartfelt gratitude and sincerest thanks to my supervisor, Mr. Abdull Halim Abdul, Lecturer in Petroleum Engineering and Geoscience Department for his undying support and encouragement, not to mention his tenacity in overseeing the completion of my dissertation.

Not only that, I would also like to offer my gratitude to AP Askury Abdul Kadir in the same department for his advice and wisdom offered in the early stages of my project and as well as my examiner on a few occasions.

Moreover, huge thanks as well to all the Lab Technicians of the aforementioned department whose names are too many to be mentioned, for their sincerest cooperation in ensuring that my experiments were executed to completion with the highest data accuracy attainable as possible.

Last but not least, token of appreciation to my friends and family for their words of encouragement during the hard and challenging times faced in this project. It made my day better on many occasions.

LIST OF FIGURES

Figure 1	General geology of Kinta Valley and surrounding areas	4
Figure 2	Typical stress strain curve	9
Figure 3	Components of stress	10
Figure 4	Principal stresses of a cube	10
Figure 5	In situ stress state in stress strain graph	11
Figure 6	Stress orientations around a fracture	11
Figure 7	World Stress Map	12
Figure 8	Map of Universiti Teknologi PETRONAS	15
Figure 9	Typical stress-strain curve	18
Figure 10	Elastic constants	18
Figure 11	Mohr circle	19
Figure 12	Stress transformation formula deriving the equation of a circle	20
Figure 13	Sample of Borehole Data I	24
Figure 14	Sample of Borehole Data II	25
Figure 15	Sample of Borehole Data III	26
Figure 16	Land Survey Contour Map	27
Figure 17	Cross Section B	28
Figure 18	Cross Section A	28
Figure 19	Percent passing (%) against diameter of sieve (mm)	31

Figure 20	Dry density (mg/m3) against moisture content (%)	32
Figure 21	CBR value (%) against moisture content (%)	33
Figure 22	Proving ring division against penetration of plunger (mm)	33
Figure 23	Triaxial test data and Mohr Circle	35
Figure 24	Triaxial test graphs	36

LIST OF TABLES

Table 1	Sieve Experiment Data for Sample A	30
Table 2	Sieve Experiment Data for Sample B	30
Table 3	Compaction / CBR Data	32

CHAPTER 1

INTRODUCTION

1.1. Background

The US National Committee on Rock Mechanics (1974) defined rock mechanics as “the theoretical and applied science of the mechanical behavior of rock and rock masses; it is that branch of mechanics concerned with the response of rock and rock masses to the force fields of their physical environment”. Brady and Brown (1993) mentioned that rock mechanics forms part of a broader topic of geomechanics which is “concerned with the mechanical responses of all geological materials, including soils. Soil mechanics involves the study of behavior of soil from small scale to a landslide scale where as rock mechanics deals mainly with petroleum industry, tunnel design, rock breakage and rock drilling.

In order to understand the processes that contribute to the failure process, we need to investigate what occurs on the small scale. Predictions of the macroscopic behavior are based upon what happens physically at the microscopic scale. Geomechanics uses a mechanistic rather than a phenomenological approach. Rock mechanics is mainly used for engineering structures analysis and to understand earth processes such as fault mechanics, lithospheric strength and propagation of seismic waves.

Drilling is a cutting process that utilizes drill bit to cut or enlarge a hole of circular cross section in solid materials. The drill bit is also known as a rotary cutting tool which is multipoint. The bit is pressed against a surface and rotated at rates of hundreds to thousands of revolutions per minute. Surface drilling is where boreholes are

collared at the surface of the earth as opposed to boreholes collared in mine workings or underwater.

Borehole logging is a process by which a probe is lowered into the borehole prior to drilling for hydrocarbon resources or water. These probes have the ability to measure the composition of soils, map the area or to provide any other relevant information. This process can produce an extremely detailed description of the area. Well logs are logs that record the results of the borehole probe. There are two types of log mainly geological and geophysical log. The former refers to the process of bringing samples to the surface of the soil for study whereas the latter refers to the log created by a special probe lowered into the borehole that gathers information passively. Bore log can be used to determine of the area contains the target minerals. Well logging tools are very sensitive and utilizes electrical currents, radioactivity, EMW and acoustics. Bore logging normally takes place from the bottom towards the top of the borehole. Geophysical logging is more precise as the geological measurements are taken on site. Since borehole logging can obtain vital information with regards to formation evaluation, it can be used for geomechanical studies. However, it is more accurate to combine it with laboratory testing to validate the results.

The study area takes place at Universiti Teknologi PETRONAS (+4° 23' 3.07", +100° 58' 8.02"), Tronoh, Seri Iskandar, Perak. It is located almost 30km south of Perak state capital, Ipoh. This area is said to be underlain by original limestone beds of the Kinta Valley, presumed to be Carboniferous or possible Permian age. The geology of Kinta Valley and its surrounding area was well-described and illustrated by Ingham & Bradford (1960, see Figure 1). It started during the Silurian time with the deposition of the clastic sediment in a relatively deep marine setting followed by the deposition of limestone following the progressive shallowing of the sea floor. This is evidence by the presence of rich shallow marine benthic organisms within the Kinta Limestone from Devonian to Permian age. Both of these clastic and calcareous Palaeozoic rock

formations were intruded by acidic igneous rocks during the Late Triassic-Early Jurassic time. This intrusion formed the Main Range, Kledang Range and Bujang Melaka Granites which comprised mainly of coarse grained porphyritic biotite granites. These are S-type granites formed due to the collision between the Sibumasu and the East Malaya Block. This intrusion was also responsible in transforming the older sedimentary rocks into marble and schist and the deposition of rich tin and iron ores during its late phase emplacement. Following the collision of Sibumasu-East Malaya, Peninsular Malaysia was uplifted to form a new terrestrial environment and to allow exogenic processes to take place. The Post Triassic exogenic geological processes have eroded weaker rocks and formed the Kinta Valley prior to the deposition of the Simpang Formation and rich plaser tin deposits and have etched the limestone to form several cock-pit and isolated tower karst with many small and large cave. This limestone beds have been severely eroded and karstified. The clastic sequence exposed in the southern part of Kinta Valley consists of alternating beds of sandstones, shale, clay or mudstone and subordinate siltstone. Reddish brown diagenetic iron oxide nodules, laminae, dendrites and fracture infill are common throughout the section. The clastic sequence in this area is most likely equivalent to Kati Beds (Ingham & Bradford, 1960). The sandstone beds can be up to several meters thick and are composed of well rounded, well sorted, medium to coarse quartz grain size with a small proportion of black grains of heavy minerals. Remains of alluvial tin mining activities mostly in forms of mine ponds are found scattered all over the Kinta alluvial plain. Today, a combination between mining remains, rehabilitated ex-mining lands, urbanize areas and the naturally preserved karstic landforms had created a rare scenic view, not seen anywhere in this region. The Kinta Valley limestone karst can be divided into cockpit karst and isolated tower karst containing many caves, valleys and natural monuments of high heritage.

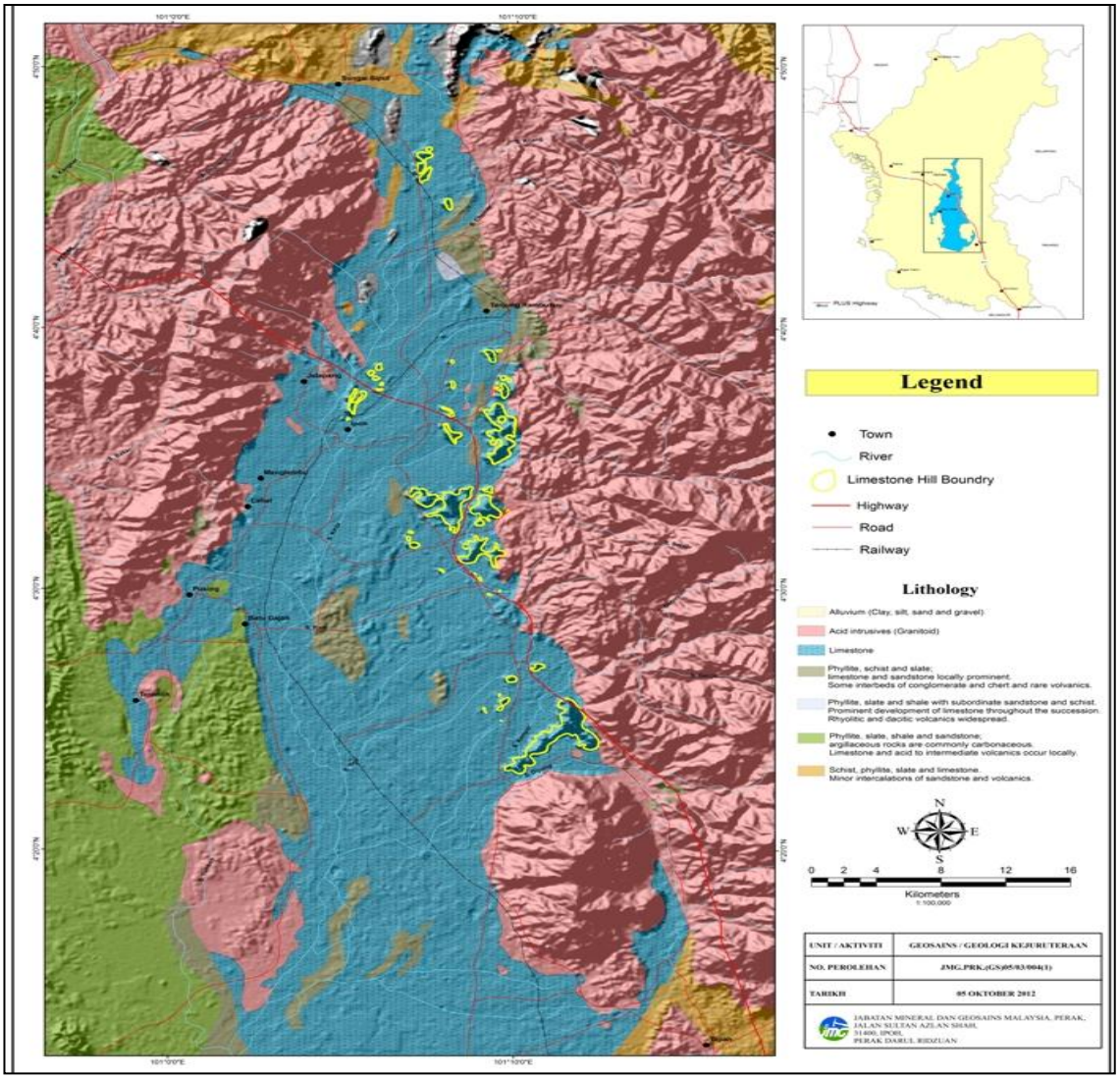

FIGURE 1. General geology of Kinta Valley and surrounding areas (Ingham, 1986).

1.2.Problem Statement

The geomechanical properties such as rock and soil compressive and shearing strength, elastic constants, porosity, particle cohesion, density, pore pressure and water saturation based on surface borehole log in the surrounding areas of Universiti Teknologi PETRONAS have not been studied before. The landscape is well developed and there exists a possibility that further construction activities might occur in the future.

Therefore, this study would assist in planning and design of any activity that is related to the strength and stability of the soil and rocks. Without proper geomechanical studies, there exists a risk in landslides, underground water contamination, building cracks and structural failures or other land deformation features such as sliding and slumping. The main research question to be answered is **"What is the geomechanical properties of the soil in the surrounding areas of Universiti Teknologi PETRONAS ?"**

1.3.Objectives and Scope of Study

This study has a sole objective to be achieved in order to answer the research questions:-

1. To study the geomechanical properties of the soil in the surrounding areas of Universiti Teknologi PETRONAS.

The scope of study involves land survey mapping to determine the elevation of the area. This information will be used to construct two cross sections as further explained in the methodology section by correlation of geological borehole logs. Laboratory tests such as CU triaxial compression test for soil, particle size distribution and compaction / CBR test will be performed.

CHAPTER 2

LITERATURE REVIEW

Application of geomechanical studies on rock and soil properties in petroleum exploration and production is based on both simple and self-evident context. First and foremost, a rock mass such as the source rock, reservoir rock and seal rock which form the basis of a petroleum system can be ascribed a set of mechanical properties that can be evidently measured in standard tests. Next, during a drilling or fracking operation especially in the exploration, appraisal and production phases, the rock structures in the subsurface will be significantly altered to both mechanical and fluid stresses. Hence, the mechanical performance of the structure is amenable to analysis utilizing the principle of classical mechanics (Brown & Brady, 1993). Thirdly, the capacity to predict the mechanical performance is vital to exert control of the rock masses in the subsurface. In a practical context, this will ultimately translate to an enhanced in the performance and production capabilities of any well concerned. This in turn will trigger higher rates of profitability which is based on the premise of cost and time savings due to significantly better understanding and also where HSE is concerned. With the big boom in unconventional reservoirs mainly shale gas and shale oil, the importance of geomechanical studies have reached new heights (Healy, 2012). With unconventional reservoirs being new, numerous countries such as China, India, Poland, Russia, US, Indonesia, Argentina, Bulgaria, Hungary, Romania, Australia and many more have placed their sights into deeper understanding of geomechanical properties of hydrocarbon reservoirs (Healy, 2012). Geomechanics can be used to study rock properties; in situ stress regime, pore fluid pressures, fault and fracture networks and failure in doing so could result in a poor model where there will be possible risks such as earthquake. A. Green et al. (2012) reported that after a fracking job at the Preese Hall -1 well in Blackpool, UK, an earthquake of about 3.0 magnitude on the Richter Scale was triggered. Further investigations concluded that they had a flawed geomechanical model of the shale reservoir and did not map a main fault line at the base. As a result, when the

fracking fluid was pumped into the well at high pressure, the fault was triggered and the surrounding fracture area was activated and propagated that caused a mass slide of rock body. Post mortem concluded that to eradicate that problem, a good geomechanical model aided by detailed fault study and seismicity has to be conducted to thoroughly assess all fracture networks within the reservoir (A. Green et al., 2012). The permeable fracture network has to be quantified and predicted in the most accurate manner possible in both clastic and carbonate reservoirs. Sandstone, shale and limestone have variable intrinsic parameters that respond very differently to stresses and strains from tectonics and induced fracturing. Thus, Healy (2012) and (Paillet, 2012) supported the notion that reliably accurate geomechanical models have to be used to predict fracture patterns to improve production capabilities. Mohiuddin, Khan, Abdulraheem, Al-Majid and Awal (2006) concluded that drillers often overlook the importance of rock mechanics in the design of directional and horizontal wells. This is because the mud weight varies with inclination and mud is vital in keeping the borehole stable during a drilling operation. The only way in doing this is to conduct a proper analysis of the in situ stresses, porosity permeability and rock strength (Sengupta, et al., 2011).

However one thing to note is that geomechanics is not only applied in the oil and gas industry, but also in the mining and construction industry. Its worldwide application severely emphasizes its importance. In rock classification, two methods can be used to study the geomechanical properties such as Rock Mass Rating (RMR) and rock mass quality index (Q) (Abdullatif, 2009). This classification, together with correlation with geomechanical studies, is effective in determining variable support requirements for excavation, construction and tunneling designs. By combining field studies with physical analysis such as point load test, uniaxial compressive strength (UCS) and poroperm tests, the RMR can then be performed by the summation of six properties which are UCS, RQD, spacing of discontinuities, condition of discontinuities, groundwater condition and orientation of discontinuities (Abdullatif, 2009). These classifications are vital especially in carbonate formations which have karst features that are engineering hazards for example failure of carbonate rocks over voids created by

dissolution or failure due to downward washing of soil into old stable voids. (Abdullatif, 2009). Abdullatif's (2009) study has some familiarity to this study due to prevalence of limestone in the Kinta Valley area. Density of carbonates increases with age while porosity will be reduced. However diagenetic processes such as dolomitization and dedolomitization can increase porosity and the variation between density and porosity often has an influence on the strength and deformation characteristics of carbonate rocks. Porosity will decrease the strength of the rock due to presence of void spaces that does not support the grains adjacent to it (Topal & Doyuran, 1997). Hussain El Hassan and Adbulraheem (2006) conducted a study that investigated the relationship between elastic constants of the reservoir and its grain size distribution. It seems that grain size has a much bigger impact than mineralogical properties of the sample (Ulusay, Turelli & Ider, 1994; Bell, Culshaw & Cripps, 1999). The data also was used to relate the reservoir quality to its depositional environment. However, it was concluded that particle size distribution (mean, median, skewness and kurtosis) did not show any significant relationships except for sands deposited in different environment where clean sand with moderate to good sorting showed lower Young's modulus and Poisson ratio (Hussain, El Hassan, & Abdulraheem, 2006). The finer sediments deposited in lagoons or offshore showed opposite results. Ulusay, Tureli and Ider (1994) conducted an almost similar study and concluded that type of contacts, grain size and shape, packing density and proximity has significant influence over engineering properties of sandstones. On the contrary, one study conducted by Jeng, Weng, Lin and Huang (2004) concluded that porosity plays a more significant role than the grain and matrix content. However they did agree that greater grain contact results in greater strength of saturated sandstones. For carbonates, a denser and finer texture would result in greater strength (Jeng, Weng, Lin, & Huang, 2004). Saturation is also shown to decrease the uniaxial compressive strengths of both weak and strong sandstones. Not only that, saturation is the key that contributes to the greatest loss of strength in a rock (Bell, Culshaw, & Cripps, 1999).

One of the fundamental concepts of geomechanics is stress. Eberhardt (2004) stated that there are three basic reasons to study and understand stresses in the context of

geomechanics. Firstly, there is a pre-existing stress state in the ground and we need to understand it as this stress state applies to analysis and design. Secondly, during a rock excavation, the stress state can change dramatically. This is because rock which previously contained stresses has been removed and loads must be redistributed. Last but not least, stress is a concept that is not familiar to many as it is a tensor quantity and tensors are not encountered in everyday life. Brady and Brown (1993) mentioned that the basics of geomechanics lie in the stress strain curve. The curve is a graphical representation of the relationship between stress and strain.

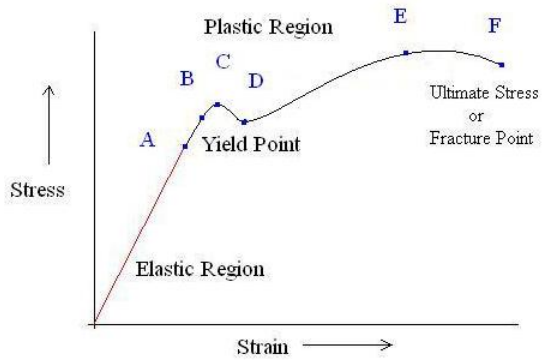

FIGURE 2. Typical stress strain curve (Brady & Brown, 1993)

(Unknown, Stress) explained the following that at the point of origin, there is no initial stress or strain in the specimen. Going up to point A, Hooke's Law is obeyed according to which stress is directly proportional to strain. Here point A is also known as the proportional limit. The straight line is known as the elastic region and the shape will revert back to its original shape after removal of stress. Moving on to point B, this curve portion is not a straight line and strain here increases at a faster rate than stress at all points. Once the curve goes beyond point B, continuous stress would cause permanent deformation. Hence point B is known as the elastic limit or yield point. The material would then go into a plastic stage till point C is reached. Starting here, the cross sectional area starts degreasing and the stress decreases to point D. Here, the workforce changes its length with very little or without any increase in stress up to point E. Point E on the graph depicts the ultimate stress. The point DE is called yielding of the material

at constant stress. From point E onwards, the strength of the material increases and requires more stress for deformation till point F. Once it reaches the ultimate stress, the point of fracture would occur at F. This point is known as the Ultimate Point or Fracture Point. Most rocks would change from brittle to ductile deformation at higher confining pressures which is about 5MPa (Bell, Culshaw, & Cripps, 1999).

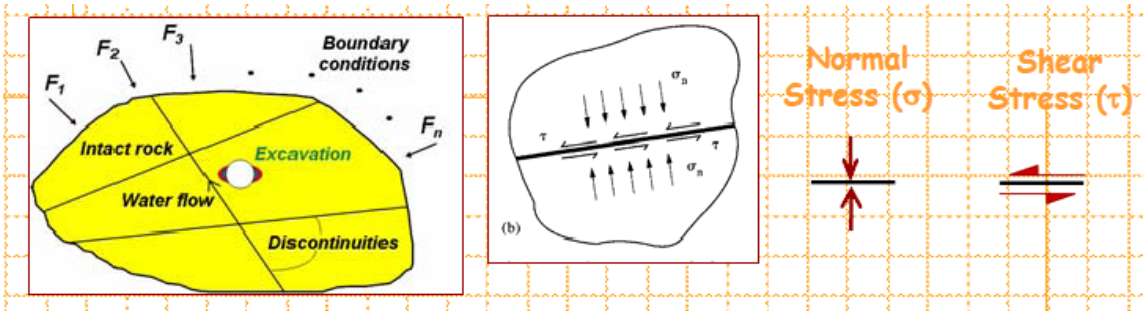

FIGURE 3. Components of stress (Eberhardt, 2004).

On a real or imaginary plane through a material, there can be both normal and shear forces. Both of these forces create the stress tensor. The shear and normal stress parameters are the normal and shear forces per unit area.

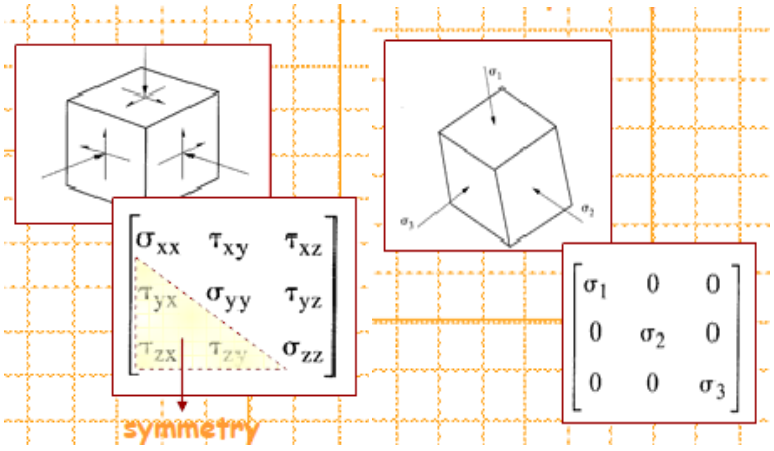

FIGURE 4. Principal stresses of a cube (Eberhardt, 2004)

The principal stresses are defined as those normal stress components that act on planes that have shear stress components with zero magnitude (Eberhardt, 2004). The actual values of the six stress components in the stress matrix for a given body subjected to the loading will depend on the orientation of the cube in the body itself. If the cube is rotated, it would be possible to find the directions in which the normal stress components take on maximum and minimum values. It is proven that in these directions the shear components on all faces of the cube becomes zero.

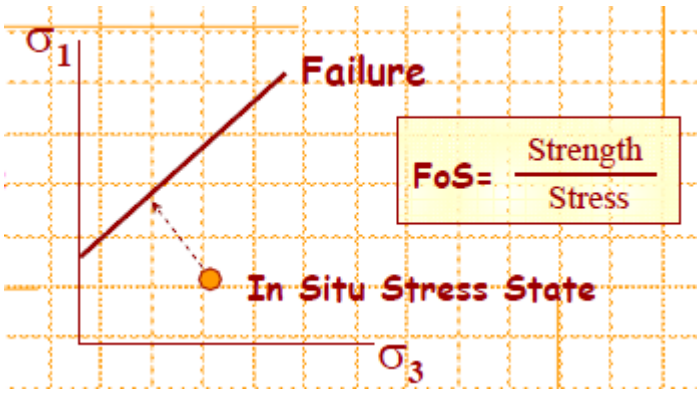

FIGURE 5. In situ stress state in stress strain graph (Eberhardt, 2004)

In situ stress has to be determined to have a basic knowledge of the stress state for example the direction and magnitude of the major principal stress and the direction in which the soil will most likely fail. When considering the loading conditions imposed on the soil mass, it must be recognized that an in situ stress state already exists in the soil. Eberhardt (2004) also pointed that in situ stresses are very common in geological structures for example fault zones act to perturb the stress field and hence the orientation and magnitudes of the principal stresses. This may lead to bias if the stress measurements are made near an isolated fracture.

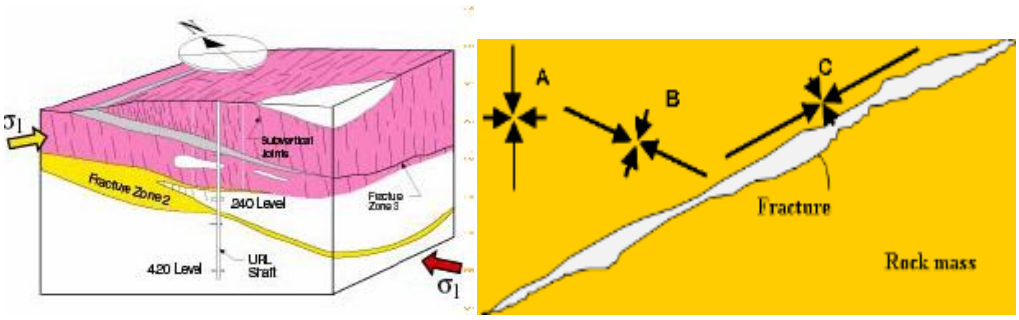

FIGURE 6. Stress orientations around a fracture (Eberhardt, 2004)

High horizontal stresses as pointed out by Eberhardt (2004) are caused by factors relating to erosion, tectonics, rock anisotropy, local effects near discontinuies and scale effects. If horizontal stresses become locked in, then the erosion/removal of overburden (that is decrease in vertical stress) will result in increase of ratio of horizontal stress to vertical stress, which is a function of Poisson ratio. Different forms of tectonic activity can produce high horizontal stresses. These horizontal stresses due to tectonics are mapped in the World Stress Map (WSM) and this map plays an important role in geomechanical studies worldwide. The mechanical earth model comprises of surfaces and faults, lithology and its petrophysical qualities, elastic properties, rock strength and in situ stresses such as overburden and pore pressure (Sengupta, et al., 2011).

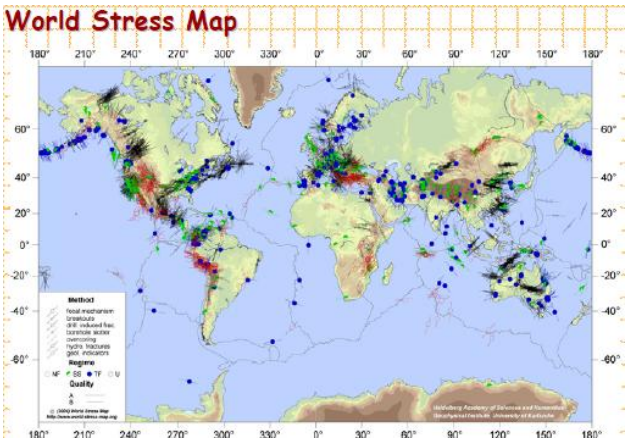

FIGURE 7.World Stress Map (Sengupta, et al., 2011)

Static mechanical properties are traditionally measured by triaxial compression tests in the laboratory. However, the prevailing factors are cost and core material availability. Hence, one alternative way is to derive the property from logging data. Static geomechanical properties can be determined from logging data once an initial model is created from the stress strain curve from laboratory results which are then calibrated with the borehole data (Franquet, 2007). Not only that, Franquet (2007) also mentioned that numerous prior experimental studies has been done and the relationship between porosity, mineralogy, bulk density, sliding crack parameters and grain contact parameters have been established and tabulated in a calibration table. These data can then be utilized with density, lithology and acoustic logs to produce a "representative rock sample" for a given depth. Using logs to predict the lithological geomechanical properties is an indirect technique but possess benefits such as lower cost and continuous estimations of mechanical properties with depths. Franquet (2007) stated that static loading differs from dynamic loading in terms of magnitude and duration where the former loading has longer duration and higher magnitude of applied stresses. To ensure the data are the most accurate, empirical relationships have to be formed between both static and dynamic for specific lithologies. In production wells where a drawdown pressure exists, the reservoir pore pressure might decrease and the porous media tries to contract (Franquet, 2007). This would cause a decrease in strain and hence be converted to a total reduction and overall horizontal stress. All of this shows that the study of mechanical properties of rock has to be aided by both mechanical tests and borehole logging tools as the correlations would allow rock deformation and failure to be forecasted from geophysical or geological data or other attributes that could be derived from those data (Birchwood, Singh, & Mese, 2008). Relationship between pore pressure and mechanical stability of bedrock is dependent on the flow of ground water in fractured rocks (Paillet, 2012). Hence, borehole data can be used to delineate the water flow by mapping the water table and hence characterize the rock mechanics of subsurface lithology (Paillet, 2012). It is known that the water table coincides with the plane of weakness of a known lithology. Well log provides access to the whole rock mass by means of a borehole and hence measurements can be made to study the in situ stress of rocks. However, Paillet (2012) also noted that measurements made in the

borehole would not be as accurate as the natural conditions due to induced fracture during drilling and possibly invaded by borehole fluids. One study was conducted at Mirror Lake, New Hampshire where fractured granitic bedrock is overlain by 10-30 meters of glacial drift. Prior studies conducted showed a strong relationship between flows of fluids in the upper layer that affected the fractured bedrock that was underlying it. The initial step was to study the fracture density on the subsurface and compare it with the findings from both the nuclear and electrical logs. This method was extremely effective in characterizing a network of interconnected fractures where a single horizontal fracture zone was found at about 50 meters of depth (Paillet, 2012). Conclusion drawn from this study was that in an extremely heterogeneous distribution of hydraulic conductivity, large scale flow paths in the subsurface cannot be delineated from a single borehole but have to be a combination of several boreholes. This delineation can be done effectively by using multiple geophysical logs and hence a geomechanical model can be constructed. The underground water flow is affected by the flow path and its localized concentration would further affect the in situ stress conditions of the rock mass.

Judging critically from the reviews, it can be concluded that grain size analysis is usually overlooked in the study of soil mechanics and should be incorporated with triaxial or uniaxial compression tests. The grain sorting - Young Modulus and Poisson Ratio relationship can be established from both the tests if done on a larger scale. If combined with engineering tests of CBR and compaction, the subgrade and soil type can be established. Combining all three data, this will significantly aid the geotechnical engineers during a construction or mining project in making decisions that will save time, costs and lives by getting the designs right the first time. Although many studies focus on rock mechanics since a substantial proportion of the subsurface consist of rocks, soil study itself can never be neglected. This is because soil, which can stretch up to several meters in the subsurface, is the “first line of defense” whenever the construction of a road or building commences. This analysis itself provides the usefulness and relevance in deepening the studies of soil mechanics which is the center of this project.

CHAPTER 3
METHODOLOGY

The purpose of this study is to study the geomechanical properties of the subsurface by correlating the borehole log data with laboratory tests data. Thus, only instrumentations related to geomechanical studies of the samples would be utilized.

As basic mapping is a requirement, the first step is to construct a land survey contour map of the area marked in the diagram below. This would require the use of a GPS to measure the coordinates and ground elevation. The data would then be recorded and tabulated. These data would then be converted into a surface contour map on an A4 paper with the appropriate scale where each contour line of different elevations would be assigned a different color. Then, using ten different surface boreholes data, two cross sections are drawn as shown in the aforementioned map. Cross section A will be about 1.8 km whereas cross section B will stretch as far as 0.733 km. Cross section A will have 6 borehole logs whereas B will have only 3 borehole logs. Each cross section will be drawn on a separate A4 size papers with appropriate scales. The lithology will be colored for better visual representation.

FIGURE 8. Map of Universiti Teknologi PETRONAS with borehole locations, cross section lines and topographic mapping area

The borehole logs are classified as entrepreneur data which are obtained from a third party at no cost. Three different laboratory tests are conducted on the sample collected. The detailed procedure and methods of data presentation and analysis are mentioned below.

- Particle Size Distribution
- CU Triaxial Compression Test for soil samples
- Compaction/ CBR Test

Particle size distribution is an important laboratory test done in many geomechanical studies to see how grain size and arrangements affect strength of the soil (Hussain, El Hassan, & Abdulraheem, 2006). It is a cheap and quick method which can be done within an hour and yield data that could be interpreted on the spot. Considering the wide variety of soil within the study area vicinity, this is a very good test to complement the triaxial compression tests results. Soil samples will be collected from borehole for testing. These same samples will be used for the triaxial compression tests. The analysis

is briefly discussed in the section below. However it has to be noted that the soil sample was brought to another location for testing due to the unavailability of the full apparatus here. The triaxial compression strength test is used for soil samples taken from the borehole. This test is effective to determine the principal effective stress, saturation build-up, consolidation stage, pore pressure dissipation, shearing stage and investigate the relationships among different variables such as:-

1. Effective shear stress with effective normal stress
2. Volume change against time
3. Pore water pressure and deviator stress against strain percentage

The compaction / CBR test is used for soil samples to measure their load bearing capacity. The relationships between dry density and moisture content; CBR% value and moisture content will be studied to determine the strength of soil. This test is mainly for qualitative analysis of soil as compared with triaxial compression tests which provide quantitative analysis of soil. This test can also be complemented with particle size distribution where maximum dry density first increases and then decreases when coarse particle content increases; and CBR value increases when coarse particle content increases as well (Wu, Wang, Liu & Ji, 2012).

CU Triaxial Compression Strength Test

1. Specimens having the shape of right circular cylinders with height ratio of two or higher are prepared.
2. Two lateral and axial deformation measurement apparatus are attached to each of the specimen.
3. The specimen is then carefully placed into the triaxial cell and a confining stress is applied and maintained by a hydraulic pump.
4. The stiff compression machine then further compresses the specimen with a spherical seating.

5. The axial stress is then applied with a constant strain rate so after about 5 – 15 minutes of loading, specimen failure will occur.
6. Purpose of the load transducer is to measure the load. Load, two axial strain and two lateral strains are recorded at a fixed interval until failure.
7. Triaxial compressive strength, σ_1 can be found by dividing the axial failure load with initial cross sectional area of the specimen.
8. For a group of Triaxial compression tests at different confining stress level, Mohr's stress circle are plotted using confining stress as σ_3 and axial stress as σ_1. Failure envelopes are determined.
9. Results should contain description of the soil, specimen anisotropy, specimen dimension, density and water content at time of test, triaxial compressive strength, stress strain curves to failure, Mohr's circle and failure envelope.

Analysis of Triaxial Compression Test

The results are represented as stress-strain curves and tabulated values of elastic constants and strength. The stress-strain data are used to calculate the compressive strength and elastic constants as mentioned below.

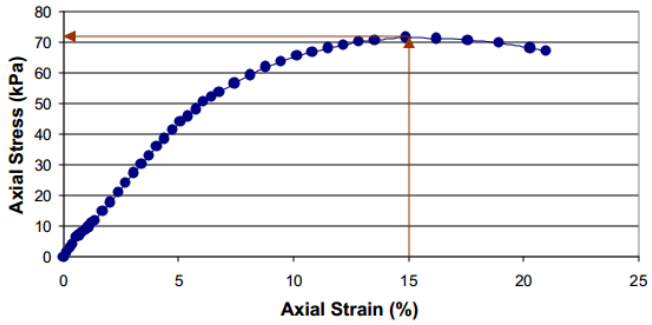

FIGURE 9. Typical stress-strain curve (Eberhardt, 2004)

In a brittle material, confined compressive strength at the confining pressure used in the triaxial test is taken as the maximum effective axial stress (total axial stress

minus percentage of pore pressure) accommodated by the sample. When strain hardening occurs, elastic constants are determined over linear sections of the stress-strain curve. Elastic constants can be calculated by using the following:-

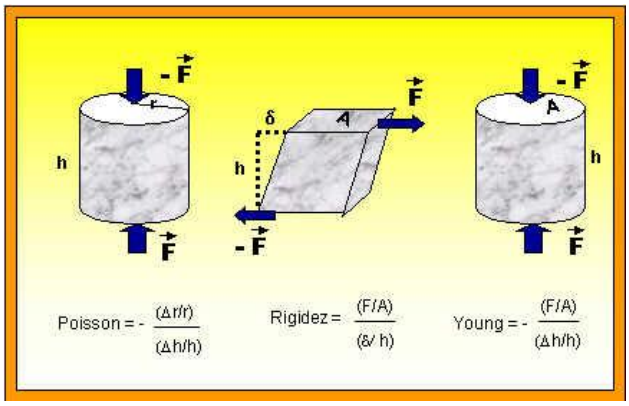

FIGURE 10. Elastic constants (Eberhardt, 2004).

Failure envelope represents the strength of a material at various values of confining pressure which could exist in situ. The Coulomb failure envelope is the simplest representation. The failure locus is a best fit tangent to Mohr's circles constructed from both triaxial and uniaxial compression tests. Mohr's circles are plotted using the effective axial and confining pressures at failure as the relevant major and minor principal stresses.

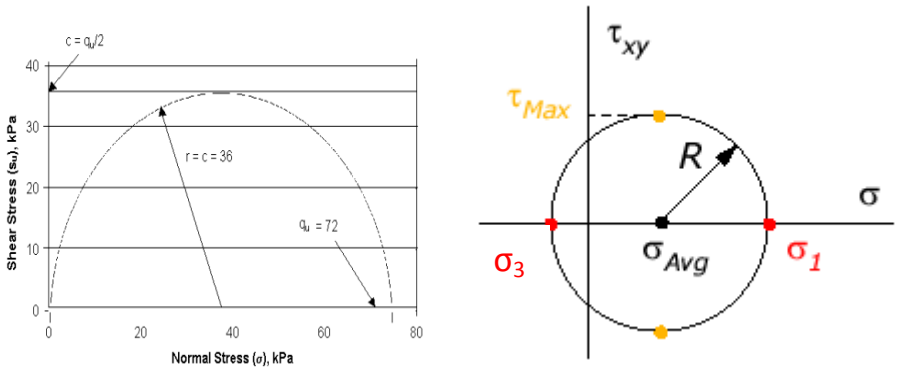

FIGURE 11. Mohr circle

The two principal stresses are shown in red which are σ_1 and σ_3 and the maximum shear stress is shown in orange, τ_{Max} and the normal stresses equal the principal stresses when the stress element is aligned with the principal directions and shear stress equals maximum shear stress when the stress element is rotated approximately 45 degrees away from the principal directions. From the graph, we can also see that as the stress elements are rotated away from the maximum shear directions, the shear and normal stress components will always lay within the Mohr Circle.

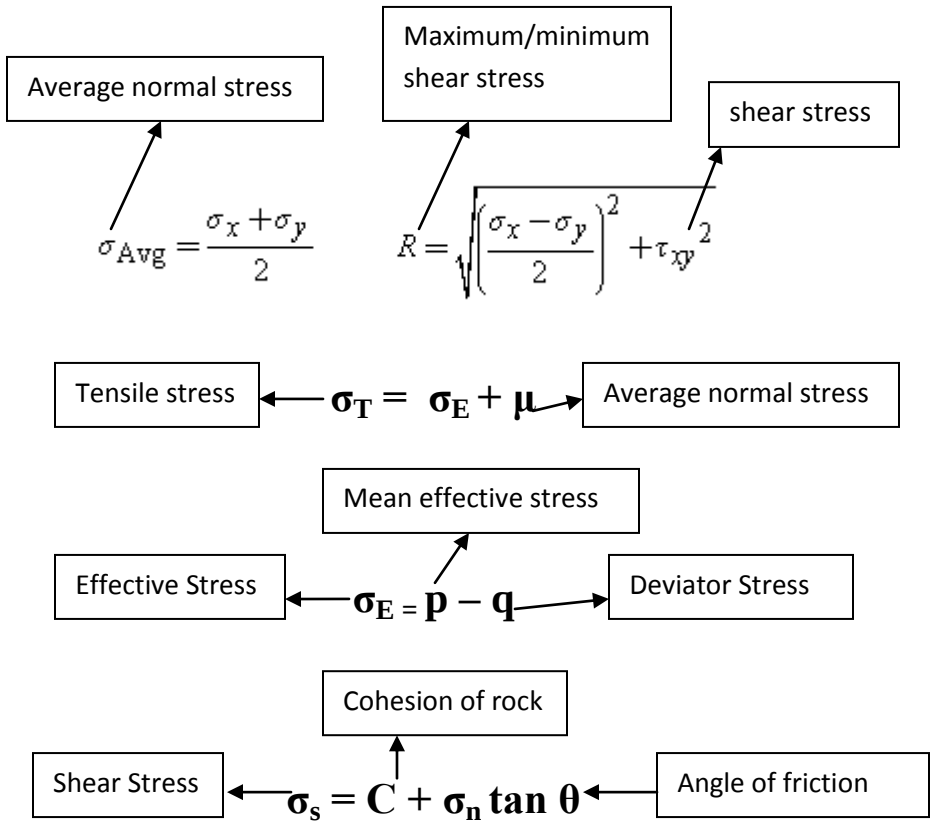

Mohr's circle can be derived by using transformation formulas for plane stress which can be rather complicated but the softwares will be deriving the values. However, the algorithm used will be as follows:-

$$\begin{cases} \sigma_{x'} - \dfrac{\sigma_x + \sigma_y}{2} = \dfrac{\sigma_x - \sigma_y}{2}\cos 2\theta + \tau_{xy}\sin 2\theta \\ \tau_{x'y'} = -\dfrac{\sigma_x - \sigma_y}{2}\sin 2\theta + \tau_{xy}\cos 2\theta \end{cases}$$

Using a basic trigonometric relation ($\cos^2 2\theta + \sin^2 2\theta = 1$) to combine the two above equations we have,

$$\left(\sigma_{x'} - \frac{\sigma_x + \sigma_y}{2}\right)^2 + {\tau_{x'y'}}^2 = \left(\frac{\sigma_x - \sigma_y}{2}\right)^2 + {\tau_{xy}}^2$$

FIGURE 12. Stress transformation formula deriving the equation of a circle

The abscissa is the normal stress and the ordinate is the shear stress. The two principal stresses are σ_x and σ_y and τ_{xy} is the maximum shear stress. Thus, we can then define the average stress, σ_{avg} and a radius R (equals to maximum shear stress).

Sieve Analysis

This test is to determine the grain size distribution curve of the given dry soil samples by passing them through a stack of sieves of decreasing mesh openings sizes and by measuring the weight retained on each sieve. Steps taken are follows:-

1. 200g of oven dried soil is obtained by weighing it on electronic balance.
2. Each sieve is weighed and cleaned. The sieve weights are recorded on the data sheets provided and then the pan is cleaned and weighed.
3. The sieves are placed in a stack of increasing aperture sizes. The largest sieve opening should be on top and the pan on the bottom.
4. The soil sample is placed in the top sieve and the cover is placed tightly on top.
5. The sieve stack is then placed into the sieve shaker.
6. The sieve shaker is turned on for 5 minutes.
7. The sieve stack is removed once the sieve shaker has stopped.
8. The sieve stack is then carefully disassembled. Care must be taken not to spill any of the soil.

9. Each sieve is weighed together with the retained soil. The weights are then recorded on the data sheet.

Compaction/ CBR Test

This test is for the evaluation of mechanical strength of soil by measuring its load-bearing capacity just under the pavement. This test is performed by measuring the pressure required to penetrate a soil sample with a plunger standard area. The measured pressure is then divided by the pressure required to achieve equal penetration on a standard crushed rock material. The procedure is as follows:-

1. Usually, 3 specimens where each weighs about 7kg must be compacted so that their compacted densities range from 95% to 100% with 10, 30 and 65 blows.
2. The empty mould is weighed.
3. Water is added to the first specimen and the 5 layers are compacted with 10 blows per layer.
4. After compaction, the collar is removed and the surface is leveled.
5. The sample is taken to measure its moisture content.
6. The weight of the mould and compacted specimen is weighed.
7. The mod is then placed in the soaking tank for 4 days.
8. Other samples are applied with different blows and the whole process is repeated.
9. After 4 days, the swell readings are measured and the percentage swell is measured.
10. The mould is removed from the tank and water is allowed to drain.
11. The specimen is then placed under a penetration piston and a surcharge load of 10lbs is placed.
12. The load is then applied and the penetration values noted.

Analysis of Compaction / CBR Test

The dry density of compacted specimen before soaking is as follows:-

$$\rho_d = \frac{M_{sas}}{V_m}$$

where:

$$M_{sac} = \frac{M_{m+ws} - M_m}{(1 + w_{ac})}$$

M_{sac} = dry mass of soil as compacted, Mg or g,
M_{m+ws} = wet mass of soil as molded plus mold mass, Mg or g
M_m = mold mass, Mg or g,
w_{ac} = water content determination of representative scraps taken during the compaction process, and
V_m = volume of mold (area of mold × initial height), a calibrate value, m^3 or cm^3.

From the collected data, a graph of dry density versus moisture content will be plotted. On the same graph, the air void lines are drawn across the compaction curve. The values of optimum moisture content and maximum dry density are obtained. Not only that, a graph of CBR percentage values will be plotted against moisture content with two parameters that is top soaked and bottom soaked. The CBR percentage can be calculated from the following:-

$$CBR = \frac{p}{p_s} \cdot 100$$

CBR = CBR [%]
p = measured pressure for site soils [N/mm²]
p_s = pressure to achieve equal penetration on standard soil [N/mm²]

Therefore as a summary, CBR test provides a qualitative analysis that can be complemented with particle size distribution analysis. On the other hand, particle size distribution analysis has to go hand in hand with triaxial compression tests for soil and rock core analysis which have been done in many studies before this.

CHAPTER 4

RESULTS AND DISCUSSION

Borehole Data

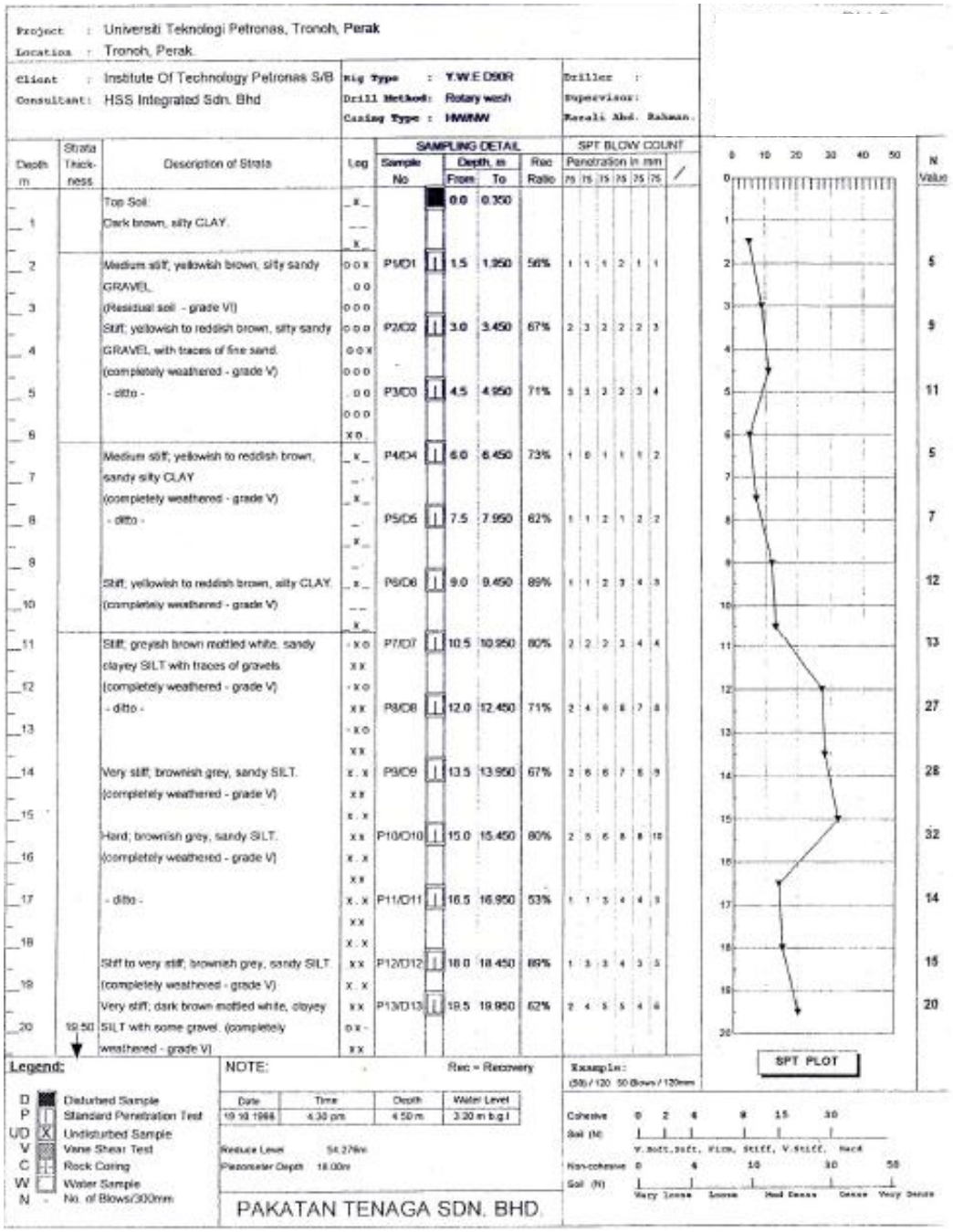

FIGURE 13. Sample of Borehole Data I

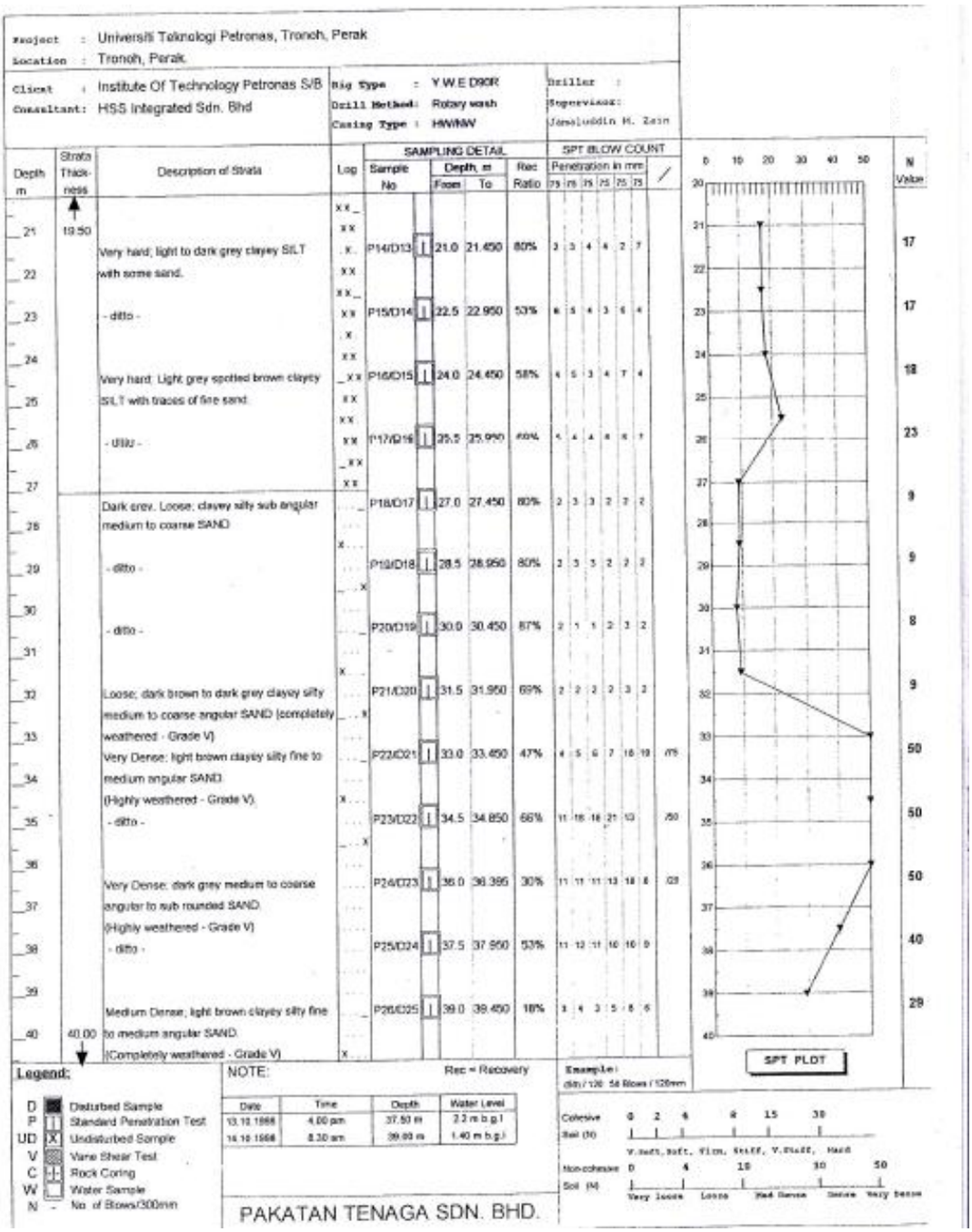

FIGURE 14. Sample of Borehole Data II

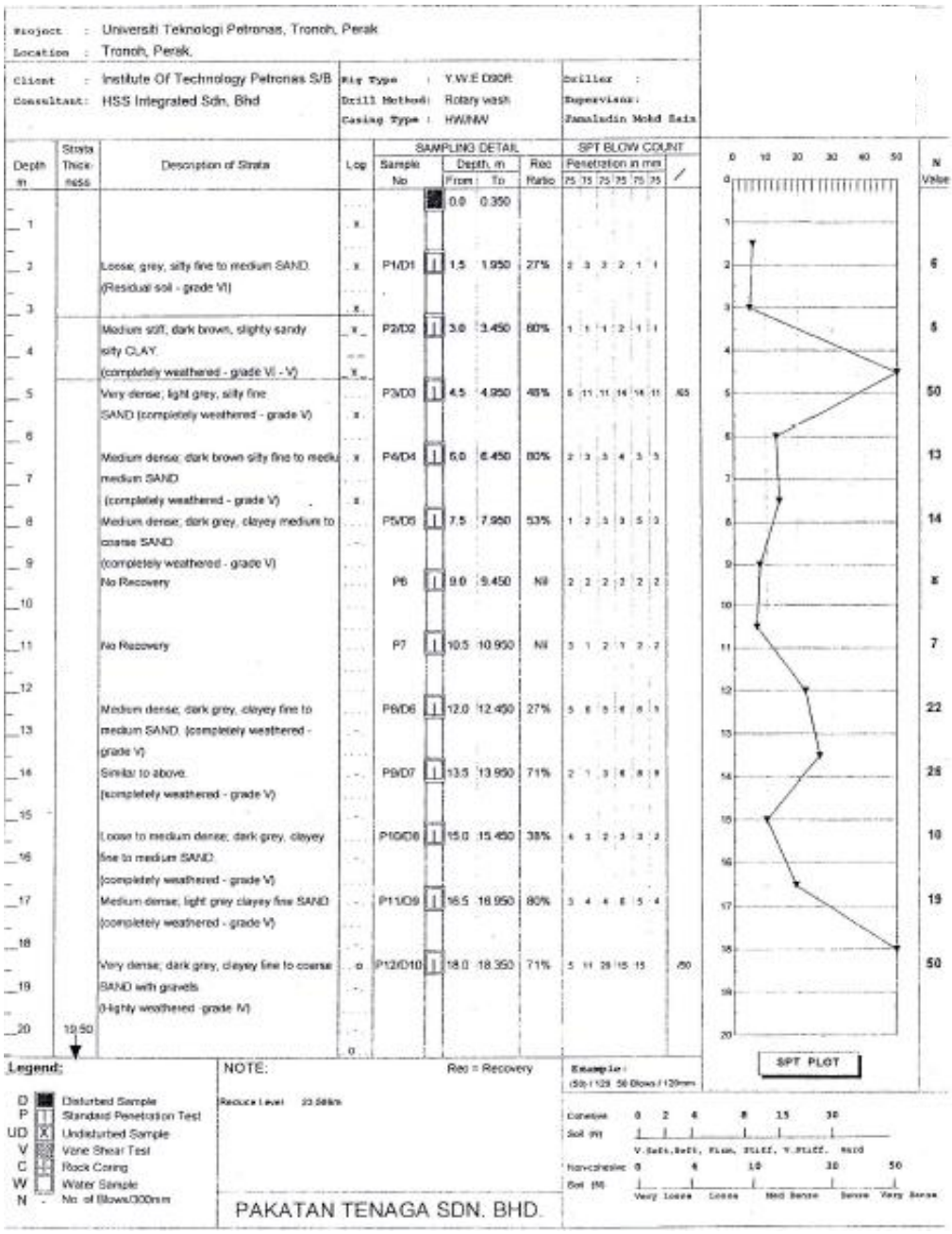

FIGURE 15. Sample of Borehole Data III

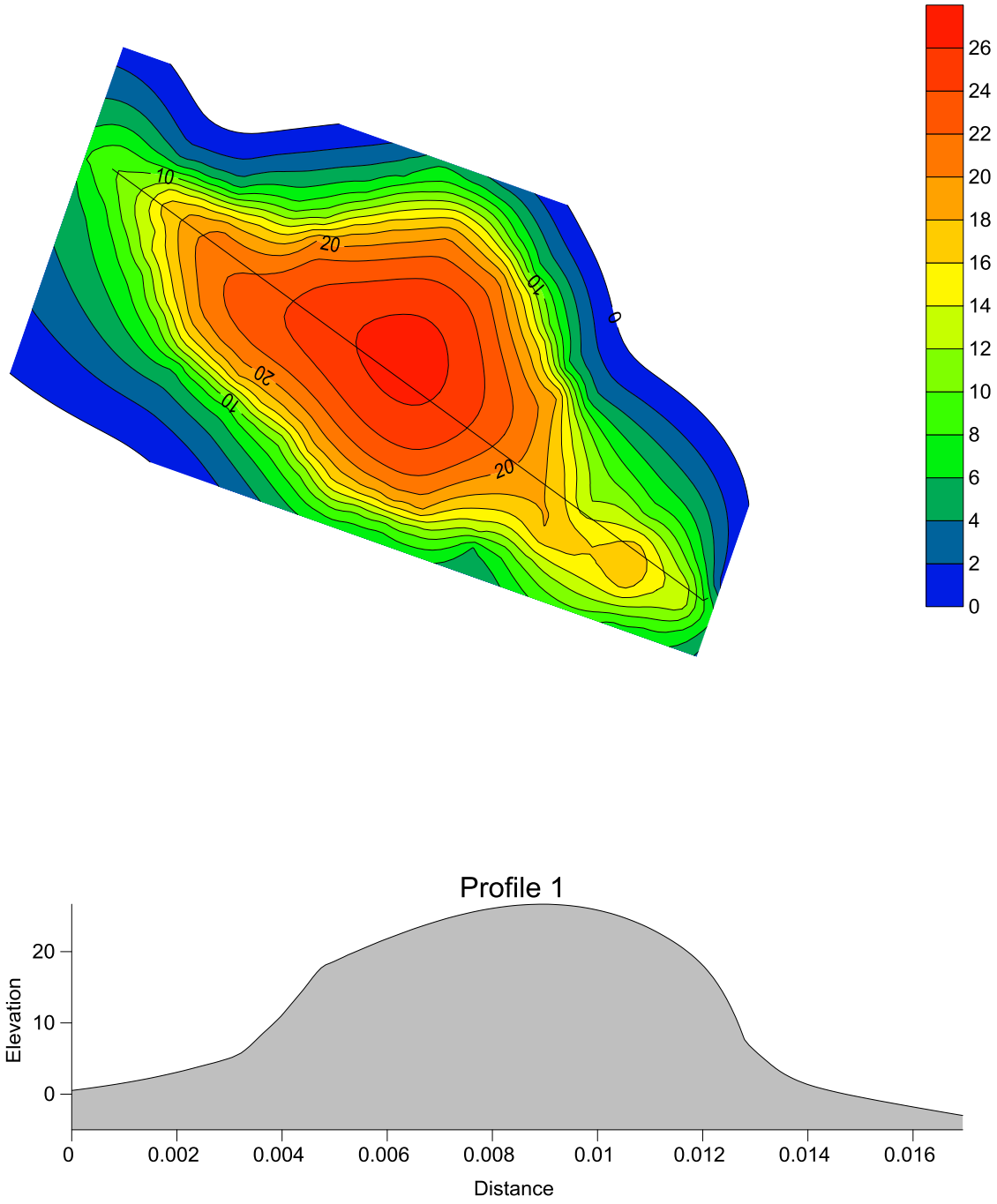

FIGURE 16. Land Survey Contour Map

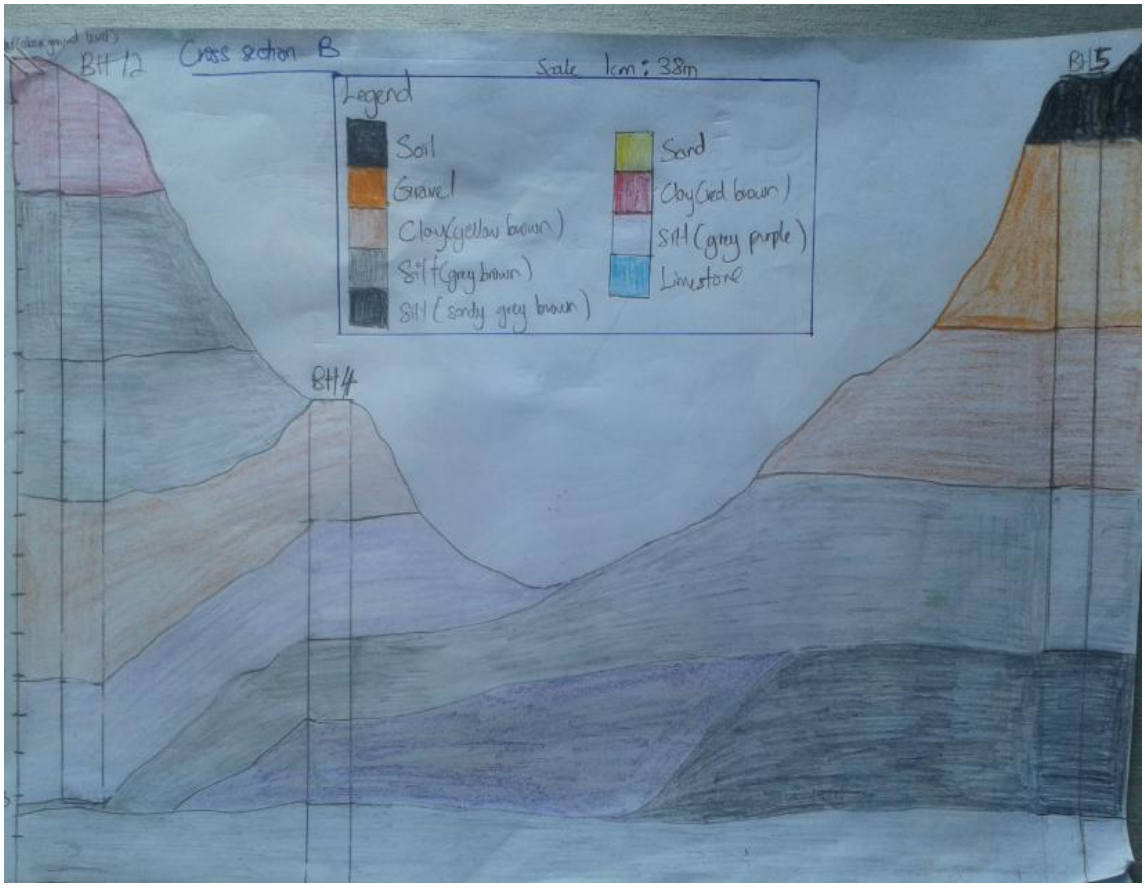

FIGURE 17. Cross Section B

FIGURE 18. Cross Section A

Based on the land survey map (FIGURE 16), the highest elevation is about 24 meters. The gradient is quite steep in the north-west direction. Borehole 2 (B2) is located around this area. There are roads adjacent to this elevated structure which could signify the topography now might differ to the past since the ground probably has to be cut and flatten in order to build roads at this vicinity. The slope of this structure looks rather man-made with built-in drainage system which could serve as a landslide mitigation step during heavy downpour. This structure, among many others in UTP, is left untouched in terms of construction-wise as probably the ground is not strong and stable enough to support buildings. As observed in borehole 2 data, the area is steep and consists mainly of clayey silt which is loose. Not only that, the naturally higher elevation also indicates that the cost to flatten or stabilize the soil would indicate higher costs. Thus it would be better to develop the surrounding areas which are of lower elevation.

Cross section B (FIGURE 17) shows that the topography starts at about 15 meters and gradually lowers towards the south east and increases again approaching borehole 5. The cross section generally shows interbedding of clay and silt about 15 meters thick. The terrain in between looks eroded and weathered. The bottom of the cross section shows that the subsurface consists mainly of silts but varies from grey-brown, sandy grey-brown to grey-purple. There is about 4 meters of gravel as seen in borehole 5 but its lateral extent cannot be seen due to lack of borehole data in between. However, even if more borehole data is obtained, there is a possibility that it has been eroded as the gravel is situated at about 12 meters from ground level and the areas adjacent to this borehole is lower in elevation.

Cross section A (FIGURE 18) shows a totally disturbed subsurface environment. Moving from west to east, the lithology shows a gradual change from silt to sand with the western region showing abundant clay and silt up to 13 meters below ground level. The base of the borehole data at about 30 meters below ground level for borehole 2 and

about 20 meters below ground level for borehole 8 indicates limestone. The presence of limestone would suggest that that the origin is of Devonian to Permian age in a deep marine setting as it belongs to the Kinta Limestone. It was deposited at the Silurian age after the deposition of clastic sediments. The silt at borehole 6 which is near the pond just a stone's throw away from the guard house is dipping downwards towards the east.

Laboratory Results

Particle Size Distribution

TABLE 1. Sieve Experiment Data for Sample A

Size (mm)	weight of soil retained (gm)	percent retained (%)	percent passing (%)
14	0	0	100
10	8.1	16.2	83.8
5	12	24	59.8
2	8.7	17.4	42.4
0.6	2.4	4.8	37.6
0.3	0.8	1.6	36
0.2	0.6	1.2	34.8
0.15	0.8	1.6	33.2
0.063	2.1	4.2	29
0.004	8.5	17	12

TABLE 2. Sieve Experiment Data for Sample B

Size (mm)	weight of soil retained (gm)	percent retained (%)	percent passing (%)
14	0	0	100
10	0	0	100
5	5.9	11.8	88.2
2	4	8	80.2
0.6	1.8	3.6	76.6
0.3	0.9	1.8	74.8
0.2	0.8	1.6	73.2
0.15	2.1	4.2	69
0.063	5.5	11	58
0.004	15	30	28

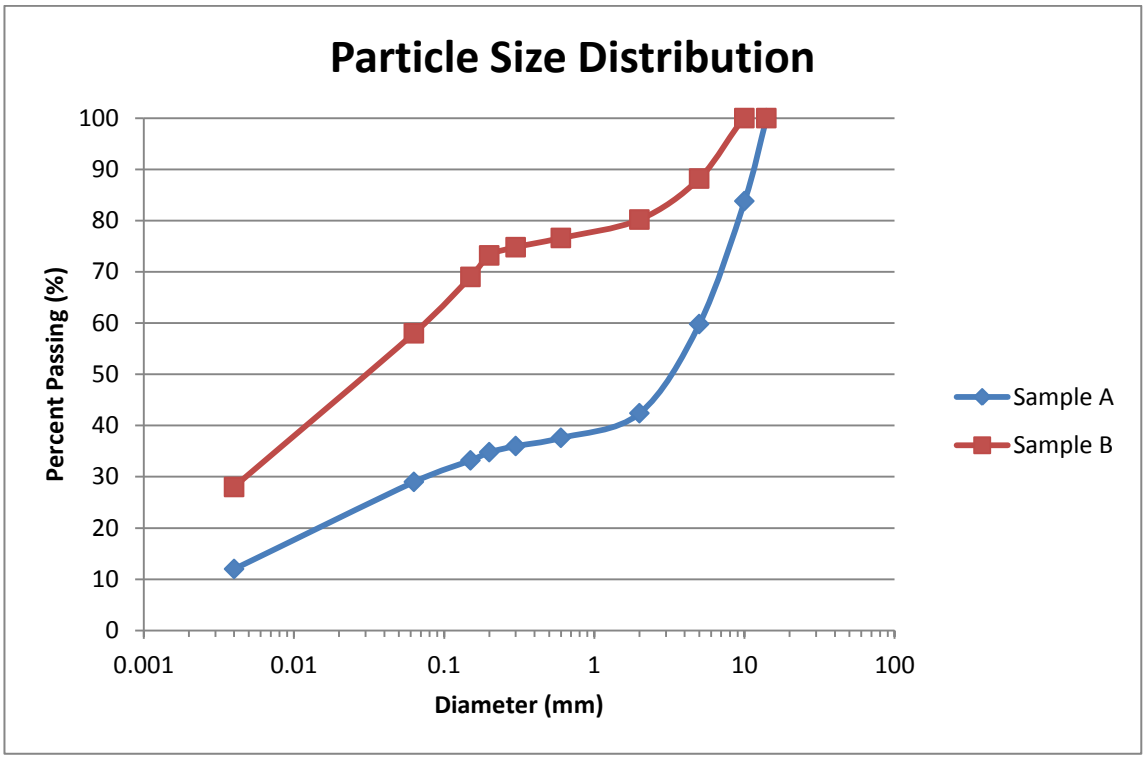

FIGURE 19. Percent passing (%) against diameter of sieve (mm)

Based on the particle size analysis (FIGURE 19), two samples were taken from borehole 5 location, one sample slightly deeper than the other. On the shallower sample, most of the composition was gravel to sand which made up of more than 50% and a small percentage of silt and clay. This observation is supported by the fact that about 18.8g of the sample has grain size larger than 2mm and the remaining from the total weight of 35.3g sample. The mode is 5.0mm which corresponds to pebbles. The median is 3mm which corresponds to granules. The mean is 4.335mm which corresponds to pebbles. The standard deviation is 2.5mm which denotes that it is poorly sorted. The skewness is 0.41. The skewness value shows that it is strongly coarse skewed.

Based on the second sample of 21g, it consists mainly of silt which is about one-third of the total constituent. Clay seems abundant as well. With comparison to the first sample, gravel here seems very little. Only 9.9g of the sample has particle sizes from 2mm to 10mm. 5.5g of the sample has size smaller than 0.063mm which is clay. Intermediate sizes from 0.150mm till 0.6mm makes up the remaining 4.7g of the sample. The median is 0.03mm which corresponds to silt. The mean is 1.01mm which corresponds to coarse sand. The mode is 5mm which corresponds to pebbles. The standard deviation is 0.75 which denotes it is moderately sorted. The skewness is 0.99 which means it is strongly fine skewed.

Compaction / CBR Test

TABLE 3. Compaction / CBR Data

Dry Density (Mg/m3)	Moisture Content (%)	CBR Value	
		Top (Soaked)	Bottom (Soaked)
1.63	11.9	10	10
1.72	15.2	12	11
1.733	18	20	12
1.65	21	5	6
1.55	24.3	1	1

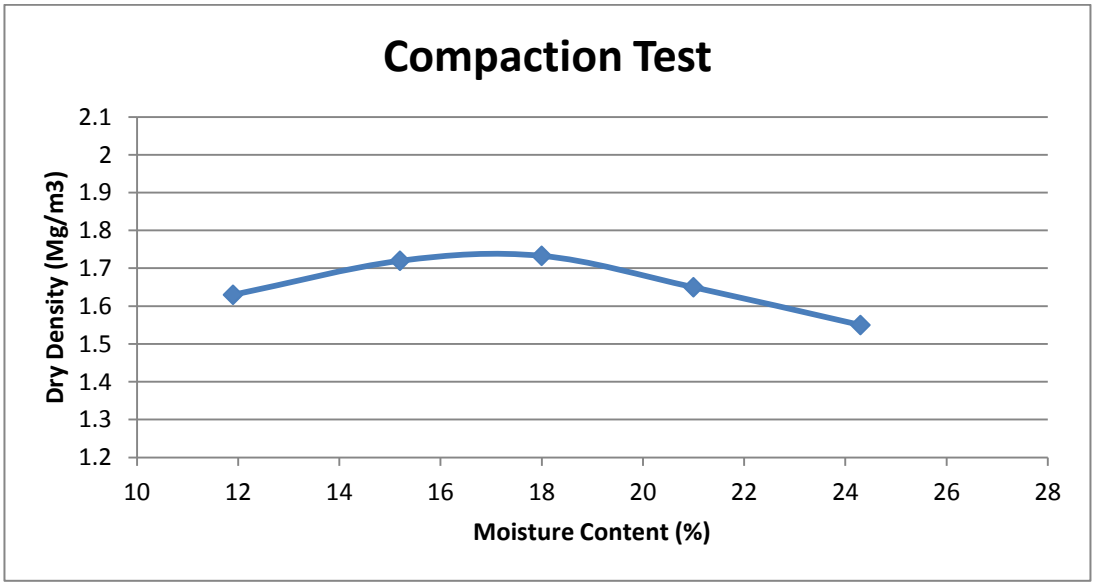

FIGURE 20. Dry density (mg/m3) against moisture content (%)

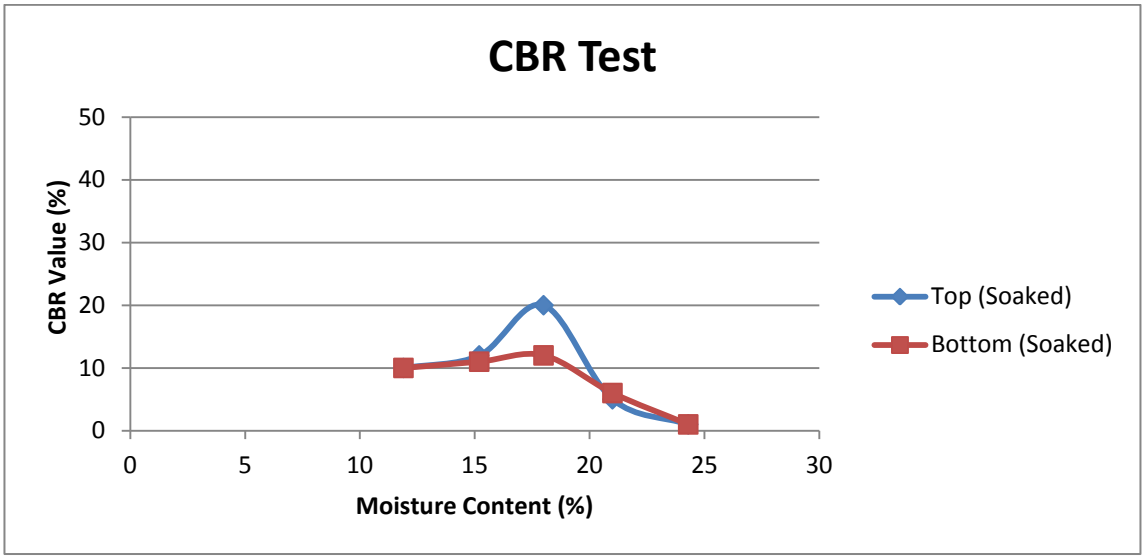

FIGURE 21. CBR value (%) against moisture content (%)

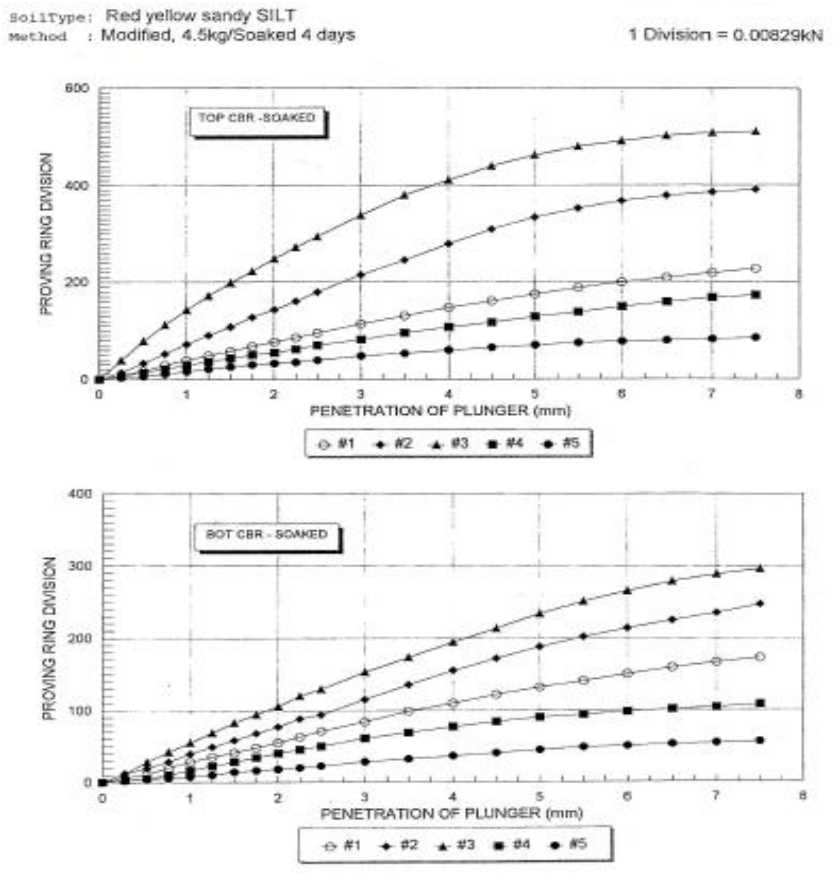

FIGURE 22. Proving ring division against penetration of plunger (mm)

As for the compaction/ CBR Test (FIGURE 20 and FIGURE 21), the same sample was used and results showed that dry density was at its highest at 1.733mg/m^3 when the moisture content was at 18%. This would indicate that the soil was at its best mechanical strength when the moisture content is at the said value. This is because with the value of 18%, the soil can be compacted best and the soil is most stable at its highest dry density. Higher dry density would mean driving out more air from the soil. Air is found in void spaces which decrease the soil strength. To properly drive all the air, optimum moisture has to be present where too little moisture is not good because grain particles will interact with each other too much and too much moisture will cause the soil to flow. The graph of CBR value against moisture content supports the notion that as the moisture content increases, the soil becomes more resistant to the plunger, hence its strength increases. However, this is only true up to 18% moisture content and beyond that, the mechanical strength of the soil decreases. The CBR value between 10% – 20% shows that the soil is mainly sand. The range also denotes a composition from clayey sand to sandy silt. Moreover, based on the graph, the top portion of the compacted soil is more towards clean sand as more force is needed to press the plunger deeper. On the other hand, the bottom portion leans towards a more clayey composition, hence requiring lesser force to press the plunger in. However, it is to be noted that there are a few drawbacks to this experiment that might affect the results. Firstly, oversized fractions (sieve size of 19mm or more) might have problems in being compacted and might yield inaccurate maximum dry densities. Nonetheless, this is not an issue as there are no oversized fractions in the sample. Secondly, soil that has particles that degrade during compaction would cause the maximum dry density to increase. This will happen to a granular – residual soil or aggregate. Hence, the value would not be representative of field conditions. Also, soil with huge proportions of large particles and lesser small particles would pose an issue in compaction due to bigger void spaces. Lastly, the competence of the personnel performing the test is also in question.

Triaxial Compression Test

EFFECTIVE CELL PRESSURE,	kN/m2	A = 20	B = 40	C = 80
INITIAL CONDITIONS				
Specimen Dimension	mm	Dia.50 x Ht.100	SPECIMEN A	SPECIMEN A
Drainage Condition		DOE	MULTI - STAGED	MULTI - STAGED
Moisture Content,	%	23		
Density Bulk	Mg/m3	1.934		
Dry	Mg/m3	1.572		
Specific Gravity	Gs	2.64		
Void Ratio,	e	0.68		
Degree of Saturation,	%	89		
SATURATION STAGE				
Final Pore Pressure Coeff,	B	1.00		
Degree of Saturation,	%	100		
CONSOLIDATION STAGE				
Initial Pore Pressure	kN/m2	495	520	559
Final Pore Pressure	kN/m2	489	490	491
Volume Change	ml	1.0	1.6	2.5
t100	min	49.0	42.3	36.0
Coeff.of Consolidation,Cv	m2/yr	83.67	97.04	113.89
Coeff.of Volume Comp, Mvi	m2/MN	0.85	0.27	0.19
K (calculated)	m/s	2.20E-08	8.17E-09	6.61E-09
LOADING STAGE		Rate of Deformation :		0.032 mm/min
Normal Load at Failure,	kN	0.1000	0.1356	0.2082
Normal Stress,	kN/m2	44.57	64.59	97.57
Cell Pressure,	kN/m2	510	530	570
Intial P.W.P.	kN/m2	490	490	490
Condition at	>>>	Max Deviator Stress	Max Deviator Stress	Max Deviator Stress
At Failure P.W.P	kN/m2	483	495	512
Effective Cell Pressure,	kN/m2	20	40	80
Minor Principal E.Stress,	kN/m2	27	35	58
Major Principal E.Stress,	kN/m2	71.57	99.59	155.57
Failure Mode		Immediate	Immediate	Immediate

Soil Type: Yellow brown sandy SILT

Effective Stress Parameters
Apparent Cohesion c ' = 2 kN/m2
Shear Angle ø ' = 26 °

Total Stress Parameters
Apparent Cohesion c = 10 kN/m2
Shear Angle ø = 18 °

NOTES: ROE = Radial One End with side drains
DOE = Drainage One End without side drains

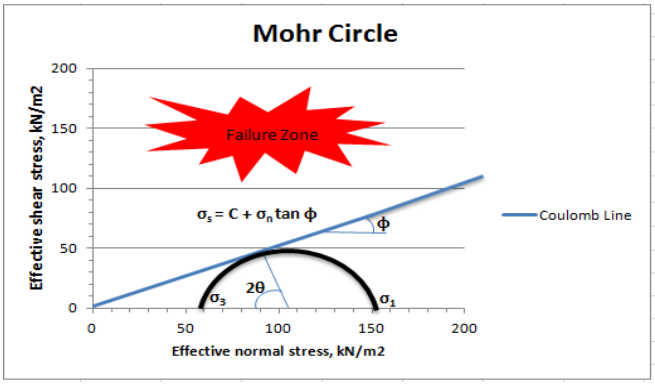

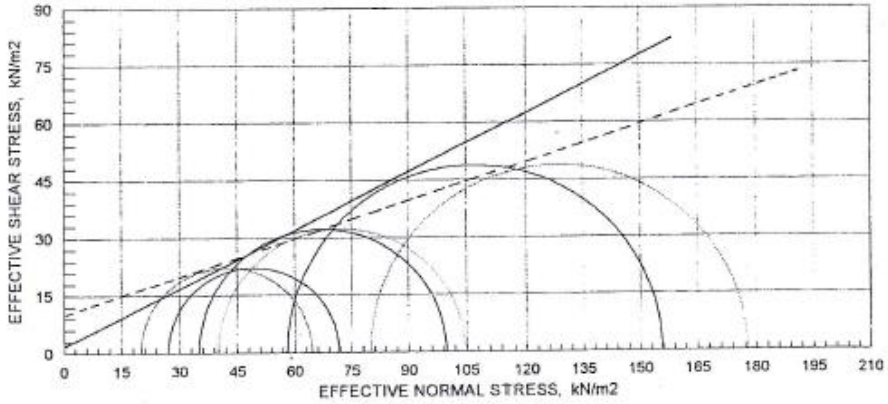

FIGURE 23. Triaxial test data and Mohr Circle

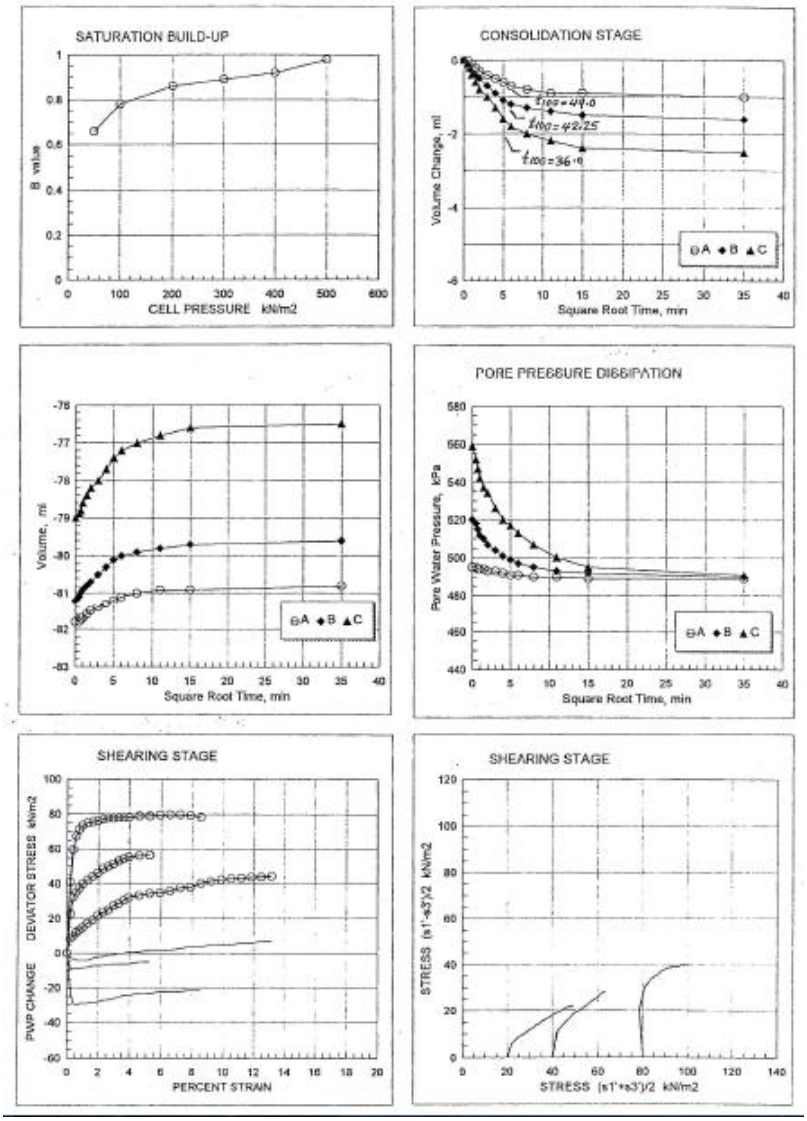

FIGURE 24. Triaxial test graphs

As for the triaxial compression test, the shear strength of a saturated soil in this test is fully dependable on the stresses applied, strain rate, time of consolidation and stress history applied on the soil. This test will measure shear characteristics under undrained conditions. The conditions are almost similar to that in the field where soils that have been unconsolidated under one set of stresses would then undergo changes in the stress regime without time for further consolidation to take place (undrained).

Hence, the field stress conditions are similar to those in the test method. Pore - water pressure measured during the test can determine the shear strength and hence express its effective stress. Drainage conditions during shearing will affect the strength parameters of soil significantly. If the sample is drained and slow shearing takes place, pore pressures will not develop and the test is called a "drained test." However, if the sample is not allowed to drain and/or shearing occurs quickly, pore pressure is developed in the specimen and the test is called an "undrained test". In soil mechanics, effective stress decreases as pore pressure increases. In the CU-bar triaxial test discussed in this report, draining did not occur during shearing, and therefore pore pressures increased and the effective stress decreased relative to the total stress. In other words, the strength parameter of the samples decreased. The fact that the drainage valve was closed during loading makes this an undrained soil experiment as opposed to drained. If A-bar had been negative, it would have been because the sample was heavily over-consolidated. The result as far as Mohr's circle is concern is that the angle of the failure envelope would have been zero because no strength gain would have occurred. Total Stress takes into account the stress based on the load which is being applied to the specimen. Effective stress takes into account total stress minus the pore pressure. The pore pressure in all three samples is increasing as the load increases, but at a slower rate. Therefore the deviator stress value for the effective stress circles is less than that for the total stress circles. Both are important in engineering analysis because it gives us a clear picture of what is taking place. With just the effective strength circles, we would not be able to assess the values or relationships between effective stress, total stress, and pore pressure.

Based on the test results, the core sample was loaded under 3 different but increasing stress conditions: 510 kN/m2, 530 kN/m2 and 570 kN/m2. However due to the pore pressure which is acting in the opposite direction, the effective cell pressure has to be calculated from simple subtraction, giving the values of 20 kN/m2, 40 kN/m2 and 80 kN/m2 respectively. The trend that can be seen is that as the effective cell pressure increases, the initial pore pressure would be higher as well. However if the core sample is allowed to settle and consolidate, some of the pore pressure dissipates through the

micro cracks or micro fractures, hence slightly reducing the value. At failure, the pore water pressure generally increases as compression is applied and this is because the pore pressure helps reduce the external stress applied hence allowing the sample to tolerate more compressional stress. However, increase in pore water pressure at similar confining pressure moves the Mohr circle towards the left as the strength of the rock is reduced. Further increment would cause hydraulic fracturing to occur which is due to tensional forces that enable cracks to open on the rock surface.

Based on the 6 graphs (FIGURE 24) constructed, some relationships can be established. Firstly, the graph of saturation build up versus cell pressure shows a linear relationship. This is because as confining pressure increases, this closes up the pores and hence lower void spaces with constant fluid volume would cause the saturation to increase. Graph of volume change against square root time shows a sensible relationship where as time goes by, the volume change becomes more apparent as the specimen is undergoing strain with a certain applied stress. Thirdly, the graph of deviator stress against percent strain shows a linear relationship as well which makes sense as when stress increases, strain increases as well. In the pore pressure dissipation graph, with increasing square root time, pore pressure gradually decreases. This is because under loading conditions, shear fracture is bound to occur, and fluid contained in the pores is able to escape, hence reducing the pore pressure with time. Based on the general shape of the Mohr circle (FIGURE 23), the sample generally undergoes compression only with the evidence being the circle is only located on the right side of the x-axis.

Sample calculation for Mohr Circle

Using circle constructed by effective cell pressure: 80kN/m^2 on yellow brown sandy silt sample as base for calculations:

σ_3 = 58kN/m^2 **σ_1 = 155.57kN/m^2**

Tangent to circle gives value of:

σ_s = 45kN/m^2 (shear stress at failure) **σ_n = 87kN/m^2**

Since **σ_3** and **σ_1** are already known from the graph, we must find angle **θ** using Coulomb law of failure formula given by: **$\sigma_s = C + \sigma_n \tan \varphi$** and **$\varphi = 90-2\theta$**

Substituting **σ_s = 45kN/m^2 & σ_n = 87kN/m^2** into the formula gives:

$45 = 2 + 87 \tan \varphi$

$\tan \varphi = 0.49$

$\varphi = 26.1°$ (angle of internal friction)

$\varphi = 90-2\theta$

$\theta = 31.95°$

The cohesion value is **2kN/m^2** which is the maximum shear stress that the soil can tolerate at zero normal stress before it fails. Higher cohesion values will raise the failure envelope higher. Here, we can conclude that if a compressive force is exerted on the sample at deviatoric stress of **97.57kN/m^2**, it will generate a maximum shear stress of **45kN/m^2** and maximum normal stress of **87kN/m^2** before failing along the plane at an angle of **31.95°**to the horizontal. The internal angle of friction is **26.1°**. The angle of friction is the resistance of the internal substance to failure. The higher the angle of friction, the stronger the sample is. This is because the higher the angle, the steeper the slope of the failure envelope and this leads to more resistance to failure. The angle value is constant for every value of cell pressure exerted on the sample where the respective shear stresses and normal stresses value changes depending on the confining pressure. Since we already have the values of **σ_3, σ_1 and θ**, we can find any values of normal and shear stresses at any confining pressure which are useful to determine the maximum

stresses the sample can tolerate before failure. For example with effective confining pressure of **40kN/m^2**, with **σ_3 = 35**, **σ_1 = 99.59 and θ = 31.95°**.

Using formula:

σ_s = ½(σ_1 - σ_3)sin(2θ) & σ_n = ½(σ_1 + σ_3) - ½(σ_1 - σ_3)cos(2θ)

σ_s = 29kN/m^2

σ_n = 53kN/m^2

From this calculations, we can conclude that at lower deviatoric stress (difference between **σ_3** and **σ_1**), it is more likely for the sample to fail. In other words, with a lower minor principal effective stress, lesser major principal effective stress is required to fail the sample. This can also be depicted on the Mohr circle where a bigger circle would mean higher strength. This sample was more consolidated due to lesser void spaces hence being able to sustain more shearing force before failing.

The effective normal stress exerted on the sample, **σ_E = p – q** where in this case **p** is the total normal stress and **q** is the pore water pressure. Pore water pressure has to be taken into account as it acts in the opposite direction of the compressional forces. Sample calculation is as follows with **q = 22 kN/m^2** and **σ_E = 97.57kN/m^2**

97.57kN/m^2 = p – 22

p = 119.57kN/m^2

Tensile stress, **σ_T = σ_E + μ** in this case is **0** as there are no tensile forces acting on the sample. It is a fully compressional forces regime. Overall, both total and effective stress strength parameters were determined from the test. The total and effective strength grew as the initial confining pressure increased. The failure envelope was defined as the best-fit-line tangent to all three samples. the Triaxial Test is a very accurate test. It can be used for CD, CU, and UU tests. The Unconfined Shear test is not a very good test and

should only be used if the project involves a relatively low load and if the budget is limited. Another implication is that strength increases as the initial confining strength increases. That means that lower in the ground the soil will be stronger because it is more confined laterally and vertically by surrounding soil. That most likely explains why soil under a footing would shear in an upside-down semi-circular shape—because the failure plane is a function of soil depth. The friction angle and the cohesion intercept were determined as well from the test results above and a sample calculation provided.

Summary of Geomechanical Data

As a summary of the geomechanical data obtained in order to make more sense: By using numerous borehole data, a cross section of the area of interest is drawn and the lithology in the subsurface noted. Based on the core samples obtained during logging and the cross section, conditions such as possible fractures, faults or salt dome or solid rocks will be determined. These data will aid in selecting the best spot to place the infrastructure. This is to ensure that the foundation deep beneath is initially solid. Then, the soil above would then be studied using three different lab tests. The particle size analysis indicates that the soil comprises of two layers, one which is mainly poorly sorted gravel to sand and slightly beneath it moderately sorted slit and clay. The grain sizes and sorting itself will tell us how the grain contact might affect the strength of the soil. In this case, both layers will have poor porosity. The top layer will have voids around gravels filled by mostly sand and some amount of clay and silt. Water retention will be lower as sands mainly do not store water and the presence of dominant gravel like materials which are harder would indicate good shear strength. On the other hand, the layer below is mainly moderately sorted silt and clay. The substantial amount of clay and silt would indicate the water retention capabilities would be higher and might flow if moisture content is too high. Also, silt and clay are mainly soft and hence are weaker compared with gravels. Higher water content would also mean high pore pressure under loading conditions and this would decrease the strength of the soil. Next, once the

engineer is wary that the top soil layer is harder and stronger than the bottom layer, the CBR and compaction values can help the engineer decide on the type and thickness of materials to be used as subgrade to overlay this particular area if a road or pavement is to be built. The subgrade would also be dependent on the presence of the two layers of soil present. Lastly, the Mohr circle failure envelope from the triaxial test would help the engineer to know about the maximum bearing load that the soil can handle before shear failure. This is a very critical piece of information to include in order to ensure that the soil is safe and will not cave in or fracture. These incidences will lead to injuries, loss of life and damage to infrastructures that will incur heavy costs. The consequences alone will prove that this study is extremely relevant and the data collected is deemed compulsory in modern day geomechanical studies.

CHAPTER 5
CONCLUSION

Universiti Teknologi PETRONAS was a former mining area with numerous man-made ponds in the east. In the western region, the topography is hillier with steep gradients up to 20 meters. Lithology-wise, clay, silt and dominates the environment up to 30 meters below ground level. Limestone on the other hand is located deeper from 30 meters onwards on the eastern region. Many areas have been flattened to accommodate construction works as can be seen at numerous man-made slopes. Bedding is fairly normal, complementing the principle of younging upwards from west to east. However, a totally disturbed soil profile at the pond area is very prominent to due to mining activities in the older days. The soil samples obtained is comprised of mainly poorly sorted gravel on the shallower depth and moderately sorted clay and silt in a slightly deeper depth. The clayey sand to sandy silt sample (CBR value from 10 - 20) located south- east to the Chancellor Hall has a maximum dry density of 1.733 mg/m^3 with optimum moisture content of 18% where its strength is at its highest. The Mohr circle plotted shows that the soil has a cohesion value of $2kN/m^2$, angle of internal friction 26.1^o where the maximum shear stress that it can handle is $45kN/m^2$ and maximum normal stress is $87kN/m^2$ before failure along the plane of 31.95^o. All these factors have to be taken into account should any activities that concern soil strength or stability is undertaken in this particular area.

REFERENCES

Abdullatif, O. (2009, November 9). Geomechanical Properties And Rock Mass Quality of the Carbonate Rus Formation, Dammam Dome, Saudi Arabia. Dhahran, Saudi Arabia.

Bell, F., Culshaw, .., & Cripps, J. (1999, January 6). A review of selected engineering geological characteristics.

Birchwood, R., Singh, R., & Mese, A. (2008, July 6). Estimating The In Situ Mechanical Properties of Sediments Containing Gas Hydrates. Houston, Texas, USA.

Brady, B., & Brown, E. (1993). *Rock Mechanics for Underground Mining Second Edition.* London: Chapman and Hall.

Eberhardt, D. E. (2004). Lecture 4: In Situ Stresses and Stress Management. *EOSC433 Geotechnical Engineering Practice and Design* . Vancouver, Canada: University of British Columbia.

Franquet, J. A. (2007, March 20). Log-based Geo-mechanical Characterization for Openhole Stability Analysis of Horizontal Wellbores. Abu Dhabi, UAE.

Free Malaysia Today. (2013, September 24). *Shale Gas, Oil Reshape World Energy Landscape*. Retrieved March 8, 2014, from www.freemalaysiatoday.com: http://www.freemalaysiatoday.com/category/world/2013/09/24/shale-gas-oil-reshape-world-energy-landscape/

Gaters III, J., Hamson III, C., Lancaster, D., & Guldry, F. (1990). In-Situ Stress Tests and Acoustic Logs Determine Mechanical Propeties and Stress Profiles in Devonian Shales.

Green, Styles, & J, B. (2012). *Preese Hall Shale Gas Fracturing Review and Recommendations for Induced Seismic Mitigation.*

Healy. (2012, July). Hydraulic Fracturing or Fracking: A Short Summary of Current Knowledge and Potential Environmental Impact. Aberdeen, United Kingdom.

Hussain, M., El Hassan, W. M., & Abdulraheem, A. (2006, July). Controls of grain size distribution on geomechanical properties of reservoir rock- A case study: Cretaceous Khafji Member, Zuluf Field, offshore Arabian Gulf.

Ingham, F. T., & Bradford, E. (1960). *The geology and mienral resources of the Kinta Valley, Perak. Geological Survey Federated Malaya 9.*

International Energy Agency. (2013). *Analysis and Studies of World Shale Gas*. Retrieved March 8, 2014, from www.eia.gov: http://www.eia.gov/analysis/studies/worldshalegas/

Jeng, F., Weng, M., Lin, M., & Huang, T. (2004, May). Influence of petrographic parameters on geotechnical properties of tertiary sandstones from taiwan.

Khulman, R., Perez, J., & Clarborne, E. (1992). Microfracture Stress Tests, Anelastic Strain Recovery and Differential Strain Analysis Assist in Bakken Shale Horizontal Drilling Program.

Mohiuddin, M., Khan, K., Abdulraheem, H., Al-Majed, A., & Awal, M. (2006, April 26). Analysis of Wellbore Instability in Vertical, Directional and Horizontal Wells.

Paillet, F. L. (2012). Application of Borehole Geophysics in Characterizing the Hydraulic and Geomechanical Properties of Fractured Crystalline Rocks. Denver, Colorado, USA.

Paradkar, A. G., Kamat, S., Gogia, A., & Kashyap, B. (n.d.). Various stages in stress strain curve of Ti-Al-Nb alloys undergoing SIMT. Hyderabad, Maharashtra, India.

R, U., K, T., & Ider, M. (1994, December). Prediction of engineering properties of a selected litharenite sandstone from its petrographic characteristics using correlation and multivariate statistical techniques.

Raj, J., Tan, D., & Abdullah, W. H. (2009). Cenozoic Stratigraphy. In C. S. Hutchinson, & D. N. Tan, *Geology of Peninsular Malaysia* (pp. 133-173). Kuala Lumpur: Universiti Malaya and Geological Society of Malaysia Publication.

Sengupta, M., Dai, J., Volterrani, S., Dutta, N., Rao, N. S., Al-Qadeeri, B., et al. (2011). Building a Seismic-Driven 3D Geomechanical Model in Deep Carbonate Reservoir. San Antonio, USA.

Sone, H. (2012, March). MECHANICAL PROPERTIES OF SHALE GAS RESERVOIR ROCKS AND ITS RELATION TO THE IN-SITU STRESS

VARIATION OBSERVED IN SHALE GAS RESERVOIRS . United States of America.

Sone, H. (2012, March). Mechanical Properties of Shale Gas Reservoir Rocks and its Relation to the In-Situ Stress Variation Observed in Shale Gas Reservoirs.

Subcommitee. (n.d.). *ASTM D4767-11 Standard Test Method for Condolidated Undrained Triaxial Compression Test for Cohesive Soils*. Retrieved April 4, 2014, from ASTM: http://www.astm.org/Standards/D4767.htm

The Star Publications. (2011, June 7). *Petronas Bet on Shale Gas*. Retrieved March 8, 2014, from www.thestar.com.

Topal, T., & Doyuran, V. (1997, February 1). Engineering geological properties and durability assessment of the Cappadocian tuff. Ankara, Turkey.

Unknown. (n.d.). *Stress*. Retrieved April 5, 2014, from TutorVista.com: http://physics.tutorvista.com/fluid-dynamics/stress.html

Unknown. (n.d.). *Triaxial and Uniaxial Compression Test*. Retrieved April 4, 2014, from KSU: http://faculty.ksu.edu.sa/Malawad/PGE%20Courses%20Info/PGE-544%20Petroleum%20Related%20Rock%20Mechanics/PGE%20544%20-%20Course%20Handout%20-%201.pdf

Unknown. (n.d.). *Unconfined Compression Test*. Retrieved April 4, 2014, from Chaoyang University of technology: http://www.cyut.edu.tw/~jrlai/CE7334/Unconfined.pdf

Wu, Y. D., Wang, W.-c., Liu, J., & Ji, K. (2012). Test research on compaction effect of expressway embankment with sand-gravel-cobble mixture. Nanjing, China.